

Properties of the exact analytic solution of the growth factor and its applications

Seokcheon Lee^{1,2} and Kin-Wang Ng^{1,2,3}

¹*Institute of Physics, Academia Sinica,
Taipei, Taiwan 11529, R.O.C.*

²*Leung Center for Cosmology and Particle Astrophysics, National Taiwan University,
Taipei, Taiwan 10617, R.O.C.*

³*Institute of Astronomy and Astrophysics,
Academia Sinica, Taipei, Taiwan 11529, R.O.C.*

Abstract

There have been the approximate analytic solution [47] and several approximate analytic forms [18, 44, 45] of the growth factor D_g for the general dark energy models with the constant values of its equation of state ω_{de} after Heath found the exact integral form of the solution of D_g for the Universe including the cosmological constant or the curvature term. Recently, we obtained the exact analytic solutions of the growth factor for both $\omega_{\text{de}} = -1$ or $-\frac{1}{3}$ [54] and the general dark energy models with the constant equation of state ω_{de} [56] independently. We compare the exact analytic solution of D_g with the other well known approximate solutions. We also prove that the analytic solutions for $\omega_{\text{de}} = -1$ or $-\frac{1}{3}$ in Ref. [54] are the specific solutions of the exact solutions of the growth factor for general ω_{de} models in Ref. [56] even though they look quite different. Comparison with the numerical solution obtained from the public code is done. We also investigate the possible extensions of the exact solution of D_g to the time-varying ω_{de} for the comparison with observations.

1 Introduction

The analysis of the luminosity distance as a function of redshift obtained from distant Type Ia supernovae discovered that the present Universe is expanding at an accelerating rate [1, 2, 3]. One of the most popular solutions to this conundrum is introducing the so called “dark energy” (DE) which is the dominant energy contribution to the present energy of the Universe with its equation of state (EOS), $\omega_{\text{de}} < -\frac{1}{3}$ (for example, [4]). The combined observations of the large scale structure (LSS) and of the cosmic microwave background (CMB) power spectra have confirmed the cosmic concordance (*i.e.* a flat universe with the present energy density contrast of the matter $\Omega_{\text{m}}^0 \simeq 0.3$ and with that of the dark energy $\Omega_{\text{de}}^0 \simeq 0.7$) [5, 6, 7, 8, 9, 10].

Due to our ignorance of the nature of the dark energy, it is practical to use the EOS of the DE, ω_{de} to characterize it [11]. Moreover, ω_{de} is the quantity constrained by cosmological observations [12, 13]. Among the excess of models, the cosmological constant Λ and a quintessence field are the most commonly proposed candidates for dark energy [14]. The former is characterized by $\omega_{\text{de}} = -1$ and the latter is a dynamical scalar field leading to a time dependent EOS, $\omega_{\text{de}}(a)$. Also models with the constant $\omega_{\text{de}} = \text{constant} \neq -1$ are important because the effects of the time varying $\omega_{\text{de}}(a)$ can be predicted by interpolating between models with constant ω_{de} [15, 16, 17, 18, 19, 20].

The origin of the current accelerating Universe is still in dispute (see for example, [21]). There are two major theories for this. One is the dark energy and the other is the modified theory of gravities (MG). However, MG are also able to be characterized by the effective EOS which is used for specifying DE models [22, 23]. Unfortunately, observations only probe the cosmological evolution of ω_{de} in an indirect way and there might be some ambiguities to differentiate DE with a specific MG model [24]. However, in most cases, while the two models give the same cosmic background expansion history $H(a)$, they predict different growth rates for cosmic LSS [23, 25, 26, 27, 28, 29].

Thus, it is important to probe the accurate background expansion history of the Universe in order to constrain the EOS of the dark energy (*i.e.* its energy density, ρ_{de}) precisely [12, 13]. Furthermore, the evolution of the matter density perturbation δ_{m} also depends on ω_{de} [16, 30, 31, 32, 33]. The formation of the LSS depends on the sound speed of the DE too [30, 32, 34, 35, 36, 37, 38]. However, in general DE models including the quintessence, the sound speed of DE is close or equal to that of light and the DE is not able to cluster on the scales of galaxy clusters and below [30, 32]. Consequently, the DE only affects the matter power spectrum on large scales ($> 100\text{Mpc}$) [16]. Usually, the LSS measurements probe scales $100\text{kpc} \sim 100\text{Mpc}$ and thus we may not need to worry about the effect of the growth of perturbation of DE when interpreting the LSS survey data.

In sub-horizon scales ($k \gg aH$), all the matter density perturbation modes $\delta_{\text{m}}(\vec{k}, a)$ grow uniformly because the dark energy do not cluster ($\Omega_{\text{de}}\delta_{\text{de}} \ll \Omega_{\text{m}}\delta_{\text{m}}$) and only the pressureless dark matter contributes to the gravitational potential. Thus, the effect of the existence of DE

appears only through the Hubble parameter, $H(a)$ and one can use the linear growth factor $D(a)$, defined by $\delta_{\text{m}}(\vec{k}, a) \propto \delta_H(\vec{k})D(a)$. From the growth factor, the growth index f (sometimes it is called as “growth rate”) is defined as $f = \frac{d \ln D(a)}{d \ln a} \equiv \Omega_{\text{m}}(a)^\gamma$ [40, 41, 42]. In a flat universe, the growth factor is obtained in the integral form for the cosmological constant Λ [43]. This solution is widely used with the approximate analytic form [44]. This solution is even extended to the general dark energy models $\omega_{\text{de}} \neq -1$ [45] by using the well known growth index parameter γ (sometimes it is called as “growth index”) given in the literature [46]. It is also known that the approximate analytic solution of $D(a)$ is obtained in the general dark energy models with the constant ω_{de} [47]. We have currently available data for $f(a)$ at various redshifts with the large degree of uncertainty though [9, 48, 49, 50, 51, 52, 53].

In what follows, we analyze in detail the recently obtained exact analytic solution of the growth factor $D(a)$ with the general constant ω_{de} dark energy in a flat universe [54, 55, 56, 57]. We note that the well known analytic solution of $D(a)$ in Ref. [47] is the approximate solution which shows the different behaviors of both $D(a)$ and $f(a)$ from the exact ones for some DE models. We do confirm that the exact analytic solutions of the growth factor with $\omega_{\text{de}} = -1$ and $-\frac{1}{3}$ obtained in Ref. [54] are the specific solutions of the exact solution of $D(a)$ for general ω_{de} given in Ref. [56] even though they look quite different. In Sec. 3, we compare the cosmological evolution of $D(a)$ obtained from the well known approximate analytic forms of it with those of the exact analytic solution $D(a)$. We also compare the values of $f(a)$ from these two solutions. We compare the exact sub-horizon solution values with the ones obtained from the full numerical values by using CMBFAST [58]. We investigate $D(a)$ and $f(a)$ with a specific parametrization of ω_{de} and its applications to observations in Sec. 4. We reach our conclusions in Sec. 5.

2 Sub-horizon scale growth factor

We use the flat Friedmann-Robertson-Walker universe to probe the sub-horizon scale linear density perturbations of matter δ_{m} in the matter dominated epoch,

$$H^2 \equiv \left(\frac{\dot{a}}{a}\right)^2 = \frac{8\pi G}{3}(\rho_{\text{m}} + \rho_{\text{de}}) = \frac{8\pi G}{3}\rho_{\text{cr}}, \quad (2.1)$$

$$2\frac{\ddot{a}}{a} + \left(\frac{\dot{a}}{a}\right)^2 = -8\pi G\omega_{\text{de}}\rho_{\text{de}}, \quad (2.2)$$

where ω_{de} is the equation of state (EOS) of dark energy, ρ_{cr} is the critical energy density, ρ_{m} and ρ_{de} are the energy densities of the matter and the dark energy, respectively. We consider the constant ω_{de} and set the present scale factor $a_0 = 1$. At sub-horizon scales ($k \gg aH$), all interesting modes of the matter density perturbation $\delta_{\text{m}}(\vec{k}, a)$ grow uniformly as long as the dark energy do not cluster [16, 31, 32]. It means that we only consider the matter perturbation in Poisson equation in this scale. Thus, the growth factor $D_g(a)$ is defined as

$$\delta_{\text{m}}(\vec{k}, a) \propto \delta_H(k)D_g(a), \quad (2.3)$$

where $\delta_H(k)$ is the scalar amplitude at the horizon crossing generated during the cosmic inflation. The alternative definition of the D_g are also commonly used (see for example, [39])

$$\delta_m(\vec{k}, a) \equiv \delta_0(k) D_g(a), \quad (2.4)$$

where $\delta_0(k)$ is the present density contrast. Then we obtain the evolution equation of $D(a)$ from the linear density perturbation equations [40, 59],

$$\frac{d^2 D}{da^2} + \left(\frac{d \ln H}{da} + \frac{3}{a} \right) \frac{dD}{da} - \frac{4\pi G \rho_m}{(aH)^2} D = 0. \quad (2.5)$$

We use D in Eq. (2.5) instead of D_g because the general solution of Eq. (2.5) does not guarantee that D is the growing mode solution. We are able to find the exact analytic solution of $D(a)$ for any value of the constant ω_{de} [54, 55, 56]. After replacing new parameters $Y = Qa^{3\omega_{de}}$ and $Q = \frac{\Omega_m^0}{\Omega_{de}^0}$ in Eq. (2.5), we obtain

$$Y \frac{d^2 D}{dY^2} + \left[1 + \frac{1}{6\omega_{de}} - \frac{1}{2(Y+1)} \right] \frac{dD}{dY} - \left[\frac{1}{6\omega_{de}^2 Y} - \frac{1}{6\omega_{de}^2 Y(Y+1)} \right] D = 0. \quad (2.6)$$

We replace a trial solution $D(Y) = cY^\alpha B(Y)$ into Eq (2.6) to get

$$Y(1+Y) \frac{d^2 B}{dY^2} + \left[\frac{3}{2} - \frac{1}{6\omega_{de}} + \left(2 - \frac{1}{6\omega_{de}} \right) Y \right] \frac{dB}{dY} + \left[\frac{(3\omega_{de} + 2)(\omega_{de} - 1)}{12\omega_{de}^2} \right] B = 0, \\ \text{when } \alpha = \frac{1}{2} - \frac{1}{6\omega_{de}}. \quad (2.7)$$

The above equation becomes the so called ‘‘hypergeometric’’ equation when we replace $X = -Y$, which has the complete solution [60]

$$B(Y) = c_1 F\left[\frac{1}{2} - \frac{1}{2\omega_{de}}, \frac{1}{2} + \frac{1}{3\omega_{de}}, \frac{3}{2} - \frac{1}{6\omega_{de}}, -Y\right] + c_2 Y^{\frac{1-3\omega_{de}}{6\omega_{de}}} F\left[-\frac{1}{3\omega_{de}}, \frac{1}{2\omega_{de}}, \frac{1}{2} + \frac{1}{6\omega_{de}}, -Y\right], \quad (2.8)$$

where F is the hypergeometric function. Thus, the exact analytic solution of the above equation (2.5) is

$$D(a) = c_1 \left(\frac{\Omega_m^0}{\Omega_{de}^0} \right)^{\frac{3\omega_{de}-1}{6\omega_{de}}} a^{\frac{3\omega_{de}-1}{2}} F\left[\frac{1}{2} - \frac{1}{2\omega_{de}}, \frac{1}{2} + \frac{1}{3\omega_{de}}, \frac{3}{2} - \frac{1}{6\omega_{de}}, -\frac{\Omega_m^0}{\Omega_{de}^0} a^{3\omega_{de}}\right] \\ + c_2 F\left[-\frac{1}{3\omega_{de}}, \frac{1}{2\omega_{de}}, \frac{1}{2} + \frac{1}{6\omega_{de}}, -\frac{\Omega_m^0}{\Omega_{de}^0} a^{3\omega_{de}}\right]. \quad (2.9)$$

$D(a)$ in Eq. (2.9) is just the general solution of the second order differential equation (2.5). Thus it does not have any physical meaning yet. It may represent the growing mode, the decaying mode or none of them before we choose the integral constants c_1 and c_2 . If we want to have the correct growing mode solution from the above analytic solution, then this solution should follow the behavior of growing mode solution at an early epoch, say $a_i \simeq 0.1$. In other words, the

ω_{de}	$\Omega_{\text{m}}^0 = 0.2$		$\Omega_{\text{m}}^0 = 0.3$		$\Omega_{\text{m}}^0 = 0.4$	
	c_{sw1}	c_{sw2}	c_{sw1}	c_{sw2}	c_{sw1}	c_{sw2}
-1/3	0.305329	0.370645	0.484579	0.546607	0.723051	0.783376
-0.8	0.563274	0.568201	0.704043	0.707640	0.845712	0.848492
-1.0	0.630418	0.631792	0.754267	0.755227	0.873819	0.874533
-1.2	0.680498	0.680868	0.790355	0.790606	0.893532	0.893715

Table 1: c_{sw1} and c_{sw2} are the values of the coefficient c_{sw} obtained from the two initial conditions of the growing mode solution, $D(a_i) \simeq a_i$ and $\left. \frac{dD_g}{da} \right|_{a_i} \simeq 1$, respectively.

coefficients of the general solution should be fixed by using the initial conditions of the growth factor,

$$D_g(a_i) \simeq a_i \quad \text{and} \quad \left. \frac{dD_g}{da} \right|_{a_i} \simeq 1. \quad (2.10)$$

After we fix the coefficients from the initial conditions, we are able to determine the growth factor $D_g(a)$ from the general form of solution $D(a)$ in Eq. (2.9). If one want to obtain the decaying mode solution $D_d(a)$ from Eq. (2.9), then one need to adopt the decaying mode initial conditions to obtain the correct coefficients

$$D_d(a_i) \simeq a_i^{-\frac{3}{2}} \quad \text{and} \quad \left. \frac{dD_d}{da} \right|_{a_i} \simeq -\frac{3}{2}a_i^{-\frac{5}{2}}. \quad (2.11)$$

Now we compare the exact growth factor in Eq. (2.9) with the well known approximate growing mode solution [47],

$$D_g^{\text{sw}} = c_{\text{sw}} \left(\frac{\Omega_{\text{m}}^0}{\Omega_{\text{de}}^0} \right)^{\frac{1}{3\omega_{\text{de}}}} aF \left[-\frac{1}{3\omega_{\text{de}}}, \frac{1}{2} - \frac{1}{2\omega_{\text{de}}}, 1 - \frac{5}{6\omega_{\text{de}}}, -\frac{\Omega_{\text{de}}^0}{\Omega_{\text{m}}^0} a^{-3\omega_{\text{de}}} \right]. \quad (2.12)$$

We rewrite the second term in Eq. (2.9) using the linear transformation formula of hypergeometric function [60],

$$\begin{aligned} & c_2 F \left[-\frac{1}{3\omega_{\text{de}}}, \frac{1}{2\omega_{\text{de}}}, \frac{1}{2} + \frac{1}{6\omega_{\text{de}}}, -\frac{\Omega_{\text{m}}^0}{\Omega_{\text{de}}^0} a^{3\omega_{\text{de}}} \right] \\ &= c_2 \frac{\Gamma \left[\frac{1}{2} - \frac{1}{2\omega_{\text{de}}} \right] \Gamma \left[1 - \frac{1}{2\omega_{\text{de}}} \right]}{\Gamma \left[1 - \frac{5}{6\omega_{\text{de}}} \right] \Gamma \left[\frac{1}{2} - \frac{1}{6\omega_{\text{de}}} \right]} \left(\frac{\Omega_{\text{m}}^0}{\Omega_{\text{de}}^0} \right)^{\frac{1}{3\omega_{\text{de}}}} aF \left[-\frac{1}{3\omega_{\text{de}}}, \frac{1}{2} - \frac{1}{2\omega_{\text{de}}}, 1 - \frac{5}{6\omega_{\text{de}}}, -\frac{\Omega_{\text{de}}^0}{\Omega_{\text{m}}^0} a^{-3\omega_{\text{de}}} \right] \\ &- c_2 \frac{\Gamma \left[-\frac{1}{2} + \frac{1}{6\omega_{\text{de}}} \right] \Gamma \left[\frac{1}{2} - \frac{1}{2\omega_{\text{de}}} \right] \Gamma \left[1 - \frac{1}{2\omega_{\text{de}}} \right]}{\Gamma \left[-\frac{1}{3\omega_{\text{de}}} \right] \Gamma \left[\frac{1}{2} - \frac{1}{3\omega_{\text{de}}} \right] \Gamma \left[\frac{1}{2} - \frac{1}{6\omega_{\text{de}}} \right]} \left(\frac{\Omega_{\text{m}}^0}{\Omega_{\text{de}}^0} \right)^{\frac{3\omega_{\text{de}}-1}{6\omega_{\text{de}}}} a^{\frac{3\omega_{\text{de}}-1}{2}} \\ &\times F \left[\frac{1}{2} - \frac{1}{2\omega_{\text{de}}}, \frac{1}{2} + \frac{1}{3\omega_{\text{de}}}, \frac{3}{2} - \frac{1}{6\omega_{\text{de}}}, -\frac{\Omega_{\text{m}}^0}{\Omega_{\text{de}}^0} a^{3\omega_{\text{de}}} \right]. \end{aligned} \quad (2.13)$$

ω_{de}	ξ	c_{sw1}	c_{sw2}	$D_{\text{sw1}}(1)$	$D_{\text{sw2}}(1)$	$D_g(1)$	$f_{\text{sw}}(a_i)$	$f(a_i)$
-0.4	-0.0486	0.589752	0.606695	0.624667	0.642613	0.631619	0.924788	0.951356
-0.8	-0.0011	0.705845	0.708663	0.733052	0.735979	0.734198	0.994917	0.998890
-1.0	0.0000	0.754267	0.755227	0.779311	0.780303	0.779699	0.998730	1.000000

Table 2: ξ , c_{sw1} , c_{sw2} , $D_{\text{sw1}}(a = 1)$, and $D_{\text{sw2}}(a = 1)$ for the different values of ω_{de} when we choose $\Omega_{\text{m}}^0 = 0.3$ and $a_i = 0.1$. $D_{\text{sw1}}(1)$ and $D_{\text{sw2}}(1)$ are the present values of the growth factors when we choose c_{sw1} and c_{sw2} , respectively. $D_g(1)$ is the present value of the exact growth factor. $f_{\text{sw}}(a_i)$ and $f(a_i)$ correspond to the initial values of the growth index obtained from D_{sw} and D_g , respectively.

Thus, $D_g^{\text{sw}}(a)$ in Eq. (2.12) becomes equal to $D_g(a)$ in Eq. (2.9) if and only if

$$c_{1g} = c_{2g} \frac{\Gamma\left[-\frac{1}{2} + \frac{1}{6\omega_{\text{de}}}\right] \Gamma\left[\frac{1}{2} - \frac{1}{2\omega_{\text{de}}}\right] \Gamma\left[1 - \frac{1}{2\omega_{\text{de}}}\right]}{\Gamma\left[-\frac{1}{3\omega_{\text{de}}}\right] \Gamma\left[\frac{1}{2} - \frac{1}{3\omega_{\text{de}}}\right] \Gamma\left[\frac{1}{2} - \frac{1}{6\omega_{\text{de}}}\right]} \quad \text{and} \quad (2.14)$$

$$c_{\text{sw}} = c_{2g} \frac{\Gamma\left[\frac{1}{2} - \frac{1}{2\omega_{\text{de}}}\right] \Gamma\left[1 - \frac{1}{2\omega_{\text{de}}}\right]}{\Gamma\left[1 - \frac{5}{6\omega_{\text{de}}}\right] \Gamma\left[\frac{1}{2} - \frac{1}{6\omega_{\text{de}}}\right]} = c_{1g} \frac{\Gamma\left[-\frac{1}{3\omega_{\text{de}}}\right] \Gamma\left[\frac{1}{2} - \frac{1}{3\omega_{\text{de}}}\right]}{\Gamma\left[-\frac{1}{2} + \frac{1}{6\omega_{\text{de}}}\right] \Gamma\left[1 - \frac{5}{6\omega_{\text{de}}}\right]}, \quad (2.15)$$

where we use the notations that c_{1g} and c_{2g} are the values of coefficients c_1 and c_2 obtained from the growing mode initial conditions in Eq. (2.10). $D_{\text{sw}}(a)$ given in Eq. (2.12) have several problems. First, $D_{\text{sw}}(a)$ contains only one integral constant c_{sw} even though it is obtained from the second order differential equation. This problem might be solved if the two integral constants in the general solution (2.9) satisfy the conditions in Eqs. (2.14) and (2.15) simultaneously. In other word, $D_{\text{sw}}(a)$ would be an exact growing mode solution if the values of c_{sw} obtained from both initial conditions (2.10) are the same. We denote that c_{sw1} and c_{sw2} are the values of c_{sw} obtained from the growing mode initial conditions $D_g(a_i) \simeq a_i$ and $\left.\frac{dD_g}{da}\right|_{a_i} \simeq 1$, respectively. As we show in Tab. 1, c_{sw1} and c_{sw2} show discrepancies for the different models. As ω_{de} decreases, the difference between the two coefficients also decreases. The same effects happen when Ω_{m}^0 is big. Thus, D_{sw} is a good approximate solution for the small value of ω_{de} and the big value of Ω_{m}^0 .

One may suspect that this discrepancy between c_{sw1} and c_{sw2} might be due to the choices of initial conditions. We investigate this as follows. The exact values of initial conditions can be obtained numerically from Eq. (2.5),

$$D_g(a_i) = a_i^{1+\xi} \quad \text{and} \quad \left.\frac{dD_g}{da}\right|_{a_i} = (1 + \xi)a_i^\xi, \quad (2.16)$$

where ξ indicates the deviation of the growth factor from the linear growth a_i at the initial epoch. We show the magnitudes of these ξ s for the different DE models in Tab. 2. In this table, we choose $\Omega_{\text{m}}^0 = 0.3$ and $a_i = 0.1$. As ω_{de} decreases, the value of ξ also decreases because there is more matter component at the initial epoch a_i for the smaller values of ω_{de} . Thus, $D_g(a_i)$ is

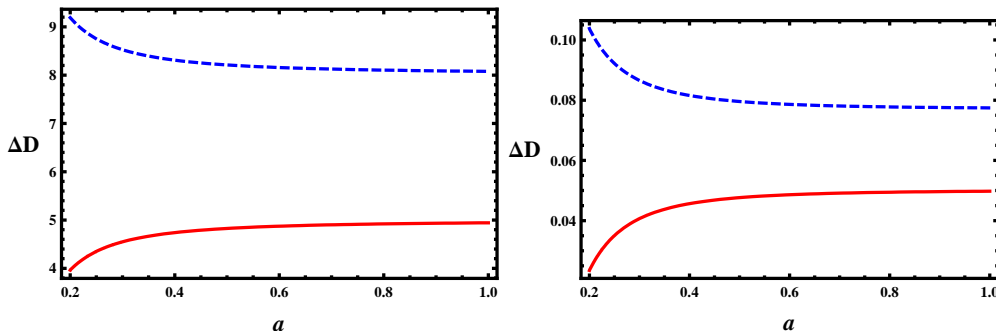


Figure 1: Errors of $D_{\text{sw}1}$ and $D_{\text{sw}2}$. a) $|D_g - D_{\text{sw}2}|/D_g \times 100$ (%) and $|D_g - D_{\text{sw}1}|/D_g \times 100$ (%) (from top to bottom) for $\omega_{\text{de}} = -0.4$ and $\Omega_{\text{m}}^0 = 0.2$. b) $|D_g - D_{\text{sw}2}|/D_g \times 100$ (%) and $|D_g - D_{\text{sw}1}|/D_g \times 100$ (%) (from top to bottom) for $\omega_{\text{de}} = -1.0$ and $\Omega_{\text{m}}^0 = 0.3$.

close to a_i for the smaller value of ω_{de} . We also shows the values of $c_{\text{sw}1}$ and $c_{\text{sw}2}$ for different DE models with initial conditions in Eq. (2.16). If we compare $c_{\text{sw}1}$ and $c_{\text{sw}2}$ values in Tab. 1 with those in Tab. 2, then we find that the discrepancies in the two values are not removed even with the exact values of initial conditions. Thus, the deviations in $c_{\text{sw}1}$ and $c_{\text{sw}2}$ are the intrinsic problem of the solution D_{sw} and irrelevant to the accuracies of initial conditions. We define $D_{\text{sw}1}$ and $D_{\text{sw}2}$ as the growth factor obtained from Eq. (2.12) when we choose the coefficient c_{sw} as $c_{\text{sw}1}$ and $c_{\text{sw}2}$, respectively. The discrepancies in the present values of the growth factor $D_{\text{sw}1}$ and $D_{\text{sw}2}$ are decreased as ω_{de} is decreased. $D_{\text{sw}}(a)$ is a good approximate solution for the small values of ω_{de} and big values of Ω_{m}^0 . We show this in Fig. 1. When ω_{de} is bigger than -1 and Ω_{m}^0 is small, $D_{\text{sw}1}$ and $D_{\text{sw}2}$ show the big discrepancies with the correct D_g as shown in the left panel of Fig. 1. The dashed, solid lines correspond to percentage errors of $(D_g - D_{\text{sw}1})/D_g$ and $(D_g - D_{\text{sw}2})/D_g$, respectively when $\omega_{\text{de}} = -0.4$ and $\Omega_{\text{m}}^0 = 0.2$. Thus, the errors at $a \geq 0.6$ are as big as 8 % and 5 % in each case. However, when ω_{de} is close and smaller than -1 and Ω_{m}^0 is big, both $D_{\text{sw}1}$ and $D_{\text{sw}2}$ are very close to D_g as shown in the right panel of Fig. 1 where we use $\omega_{\text{de}} = -1.0$ and $\Omega_{\text{m}}^0 = 0.3$. The lines indicate same percentage errors as in the left panel of Fig. 1. As shown in the figure, the errors are sub percentages in this case.

Second, one is not able to separate the growing mode solution and the decaying mode solution in $D(a)$. So far, there are only two known possible cases for separating the two modes when $\omega_{\text{de}} = -\frac{1}{3}$ and -1 [61]. This separation is impossible for general values of ω_{de} as shown above. Thus, D_{sw} is not the correct growing mode solution. $D(a)$ itself in Eq. (2.9) is the solution of the equation (2.5), and this solution cannot be separated as the growing mode solution or the decaying one. As we explained in the above, after we obtain the general solution of the equation (2.5), the solution $D(a)$ can be interpreted as the growing or the decaying mode solution by applying the

appropriate initial conditions given in Eqs. (2.10) and (2.11) to the general solution in Eq. (2.9).

The third problem is related to the growth index $f = \frac{d \ln D}{d \ln a}$. If we choose D_{sw} as the growing mode solution, then the growth index becomes

$$f_{\text{sw}} = \frac{d \ln D_{\text{sw}}}{d \ln a} = \frac{\ln \left[a F \left[-\frac{1}{3\omega_{\text{de}}}, \frac{1}{2} - \frac{1}{2\omega_{\text{de}}}, 1 - \frac{5}{6\omega_{\text{de}}}, -\frac{\Omega_{\text{de}}^0}{\Omega_{\text{m}}^0} a^{-3\omega_{\text{de}}} \right] \right]}{d \ln a}. \quad (2.17)$$

Since D_{sw} has only one coefficient, the growth index obtained from D_{sw} is independent of c_{sw} . If we choose the exact values of initial conditions given in Eq. (2.16), then the value of the growth index at the initial epoch will become

$$f(a = a_i) = 1 + \xi + \mathcal{O}(\xi^3) + \dots. \quad (2.18)$$

Therefore, $f_{\text{sw}}(a = a_i)$ is not same as $f(a_i)$ given in Eq. (2.18). This problem also happens when we choose the approximate initial conditions (2.10). Thus, the value of the growth index obtained from D_{sw} shows the intrinsic discrepancies with that obtained from the correct growth factor D_g as shown in Tab. 2. We find that the present value of f for $\Omega_{\text{m}}^0 = 0.4$ should be close to 0.6 independent of ω_{de} and thus Fig. 3 in Ref. [47] is incorrect.

Recently, we have also obtained the exact analytic solution of $D(a)$ for $\omega_{\text{de}} = -1$ [54]. There we have found that the solution of D_g for $\omega_{\text{de}} = -1$ is given by

$$D_g^L(a) = c_1^L Q^{\frac{2}{3}} a^{-2} F \left[1, \frac{1}{6}, \frac{5}{3}, -Qa^{-3} \right] + c_2^L \sqrt{1 + Qa^{-3}}. \quad (2.19)$$

The form of $D_g^L(a)$ looks quite different from $D_g(a)$ in Eq. (2.9). However, when $\omega_{\text{de}} = -1$, the general solution $D(a)$ becomes

$$\begin{aligned} D(a)|_{\omega_{\text{de}}=-1} &= c_1 \left(\frac{\Omega_{\text{m}}^0}{\Omega_{\text{de}}^0} \right)^{\frac{2}{3}} a^{-2} F \left[1, \frac{1}{6}, \frac{5}{3}, -\frac{\Omega_{\text{m}}^0}{\Omega_{\text{de}}^0} a^{-3} \right] + c_2 F \left[\frac{1}{3}, -\frac{1}{2}, \frac{1}{3}, -\frac{\Omega_{\text{m}}^0}{\Omega_{\text{de}}^0} a^{-3} \right] \\ &= c_1 \left(\frac{\Omega_{\text{m}}^0}{\Omega_{\text{de}}^0} \right)^{\frac{2}{3}} a^{-2} F \left[1, \frac{1}{6}, \frac{5}{3}, -\frac{\Omega_{\text{m}}^0}{\Omega_{\text{de}}^0} a^{-3} \right] + c_2 F \left[-\frac{1}{2}, \frac{1}{3}, \frac{1}{3}, -\frac{\Omega_{\text{m}}^0}{\Omega_{\text{de}}^0} a^{-3} \right] \\ &= c_1 \left(\frac{\Omega_{\text{m}}^0}{\Omega_{\text{de}}^0} \right)^{\frac{2}{3}} a^{-2} F \left[1, \frac{1}{6}, \frac{5}{3}, -\frac{\Omega_{\text{m}}^0}{\Omega_{\text{de}}^0} a^{-3} \right] + c_2 \sqrt{1 + \frac{\Omega_{\text{m}}^0}{\Omega_{\text{de}}^0} a^{-3}} = D_g^L(a), \end{aligned} \quad (2.20)$$

where we use the relation $F[j, k, j, -Y] = F[k, j, j, -Y] = \sqrt{1+Y}$ in the second and the third equalities [60]. Thus, the solution $D_g^L(a)$ given in Eq. (2.19) is one of the particular solutions of $D(a)$ when $\omega_{\text{de}} = -1$. We are also able to obtain the particular solution of $D(a)$ when $\omega_{\text{de}} = -\frac{1}{3}$ by using the same relation.

$$D(a)|_{\omega_{\text{de}}=-\frac{1}{3}} = c_1 \left(\frac{\Omega_{\text{m}}^0}{\Omega_{\text{de}}^0} \right) a^{-1} F \left[2, -\frac{1}{2}, 2, -\frac{\Omega_{\text{m}}^0}{\Omega_{\text{de}}^0} a^{-1} \right] + c_2 F \left[1, -\frac{3}{2}, 0, -\frac{\Omega_{\text{m}}^0}{\Omega_{\text{de}}^0} a^{-1} \right]$$

$$\begin{aligned}
&= c_1 \left(\frac{\Omega_m^0}{\Omega_{\text{de}}^0} \right) a^{-1} \sqrt{1 + \frac{\Omega_m^0}{\Omega_{\text{de}}^0} a^{-1}} + c_2 F \left[1, -\frac{3}{2}, 0, -\frac{\Omega_m^0}{\Omega_{\text{de}}^0} a^{-1} \right] \\
&= c_1 \left(\frac{\Omega_m^0}{\Omega_{\text{de}}^0} \right) a^{-1} \sqrt{1 + \frac{\Omega_m^0}{\Omega_{\text{de}}^0} a^{-1}} \\
&+ c_2 \left(-1 - 3 \frac{\Omega_m^0}{\Omega_{\text{de}}^0} a^{-1} + 3 \frac{\Omega_m^0}{\Omega_{\text{de}}^0} a^{-1} \sqrt{1 + \frac{\Omega_m^0}{\Omega_{\text{de}}^0} a^{-1}} \operatorname{arctanh} \left[\sqrt{\frac{\Omega_m^0}{\Omega_{\text{de}}^0} a^{-1}} \right] \right), \quad (2.21)
\end{aligned}$$

where $\operatorname{arctanh}$ is the inverse hyperbolic tangent function.

3 Comparison with known approximate solutions

There are several well known approximate analytic forms of the growth factor [18, 44, 45]. For the cosmological constant (*i.e.* $\omega_{\text{de}} = -1$), the well known approximate form of the growth factor at present is given by [44]

$$D_{\text{cpt}}^0 = \frac{5\Omega_m^0}{2} \left[\left(\Omega_m^0 \right)^{\frac{4}{7}} - \Omega_\Lambda^0 + \left(1 + \frac{\Omega_m^0}{2} \right) \left(1 + \frac{\Omega_\Lambda^0}{70} \right) \right]^{-1}, \quad (3.1)$$

where Ω_Λ^0 is the present value of the energy density contrast ($\rho_\Lambda^0/\rho_{\text{cr}}^0$) of the cosmological constant Λ . One is not able to obtain the growth index from the D_{cpt}^0 because it is a constant. Thus, the approximate analytic form of the growth index f_{lahav} is given separately in Ref. [42] :

$$f_{\text{lahav}}(a) = \left[\frac{\Omega_m(a)}{\Omega_m(a) + \Omega_\Lambda(a)} \right]^{\frac{4}{7}}. \quad (3.2)$$

The above solution is generalized to any value of a in Ref. [18] :

$$D_{\text{cpt}}(a) = \frac{5\Omega_m(a)}{2} a \left[\left(\Omega_m(a) \right)^{\frac{4}{7}} - \Omega_\Lambda(a) + \left(1 + \frac{\Omega_m(a)}{2} \right) \left(1 + \frac{\Omega_\Lambda(a)}{70} \right) \right]^{-1}. \quad (3.3)$$

We compare this solution D_{cpt} with the exact one in Eq. (2.20).

We show the relative errors of D_{cpt} and f_{cpt} compared to the exact solutions D_g and f when $\Omega_m^0 = 0.2$ and 0.3 in Fig. 2. The errors of the analytic approximate solution D_{cpt} are smaller than 1 % as shown in the left panel of Fig. 2. The dashed and solid lines are $|D_g - D_{\text{cpt}}|/D_g \times 100$ (%) when $\Omega_m^0 = 0.2$ and 0.3 , respectively. $f_{\text{cpt}}(a)$ is also obtained from D_{cpt} in Eq. (3.3). We compare the evolution of f_{cpt} with that of f in the right panel of Fig. 2. The solid line describes the correct f obtained from D_g . The dotted line shows the evolution f_{cpt} obtained from D_{cpt} . The error of f_{cpt} at present is about 4 % only when we use $\Omega_m^0 = 0.3$.

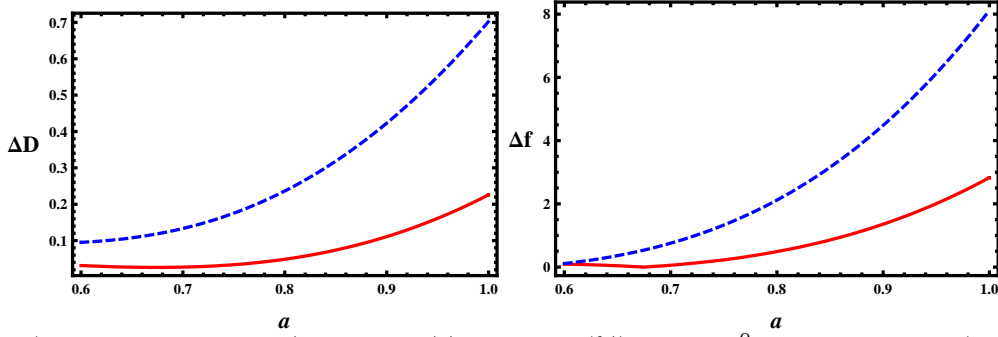


Figure 2: a) Relative errors of $|D_g - D_{\text{cpt}}|/D_g \times 100$ (%) when $\Omega_m^0 = 0.2$ and 0.3 (from top to bottom). b) Relative errors of $|f - f_{\text{cpt}}|/f \times 100$ (%) when $\Omega_m^0 = 0.2$ and 0.3 (from top to bottom).

There is also another approximate analytic solution D_{bp} for the general values of ω_{de} [18, 45]. This solution is obtained from the well known parametrization of the growth index and its parameter in Ref. [46],

$$f = \frac{d \ln D_g}{d \ln a} = \Omega_m(a)^{\gamma_{\text{ws}}}, \quad (3.4)$$

$$\text{where } \gamma_{\text{ws}} \simeq \frac{3(1 - \omega_{\text{de}})}{5 - 6\omega_{\text{de}}} + \frac{3}{125} \frac{(1 - \omega_{\text{de}})(1 - \frac{3\omega_{\text{de}}}{2})}{(1 - \frac{6\omega_{\text{de}}}{5})^3} (1 - \Omega_m(a)). \quad (3.5)$$

The approximate growth factor D_{bp} is known as the extension of D_{cpt} in Eq. (3.3) for the general ω_{de} and is given by [45]

$$D_{\text{bp}}^0(a) = \frac{5\Omega_m^0}{2} a \left[(\Omega_m^0)^{\gamma_{\text{ws}}^0} - \Omega_{\text{de}}^0 + \left(1 + \frac{\Omega_m^0}{2}\right) (1 + \mathcal{A}\Omega_{\text{de}}^0) \right]^{-1}, \quad (3.6)$$

where γ_{ws}^0 is the approximate form of the growth index parameter by choosing $\Omega_m(a) = \Omega_m^0$ in Eq. (3.5) and \mathcal{A} is the fitting coefficient in Ref. [18, 45]

$$\gamma_{\text{ws}}^0 \simeq \frac{3(1 - \omega_{\text{de}})}{5 - 6\omega_{\text{de}}} + \frac{3}{125} \frac{(1 - \omega_{\text{de}})(1 - \frac{3\omega_{\text{de}}}{2})}{(1 - \frac{6\omega_{\text{de}}}{5})^3} (1 - \Omega_m^0), \quad (3.7)$$

$$\mathcal{A} \simeq 1.742 + 3.343\omega_{\text{de}} + 1.615\omega_{\text{de}}^2 \quad \text{when } \omega_{\text{de}} \geq -1 \quad (3.8)$$

$$\simeq -\frac{0.28}{\omega_{\text{de}} + 0.08} - 0.3 \quad \text{when } \omega_{\text{de}} < -1. \quad (3.9)$$

Again the above solution D_{bp}^0 is generalized as [18]

$$D_{\text{bp}}(a) = \frac{5\Omega_m(a)}{2} a \left[(\Omega_m(a))^{\gamma_{\text{ws}}} - \Omega_{\text{de}}(a) + \left(1 + \frac{\Omega_m(a)}{2}\right) (1 + \mathcal{A}\Omega_{\text{de}}(a)) \right]^{-1}. \quad (3.10)$$

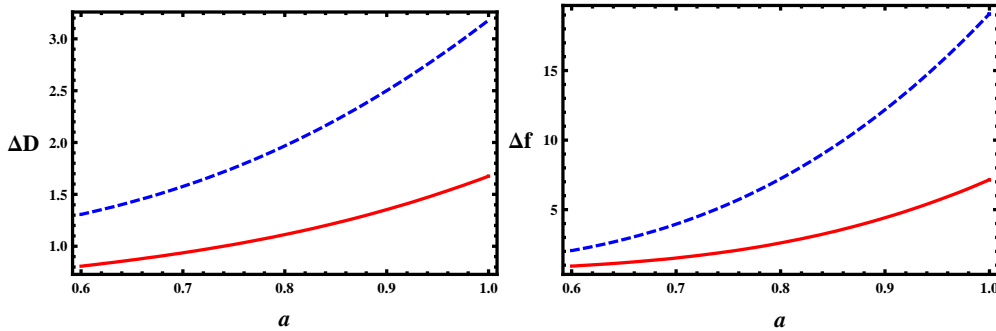


Figure 3: a) Relative errors of $|D_g - D_{\text{bp}}|/D_g \times 100$ (%) when $\Omega_m^0 = 0.2$ and 0.3 (dashed and solid lines, respectively) for $\omega_{\text{de}} = -0.8$. b) Relative errors of $|f - f_{\text{bp}}|/f \times 100$ (%) (with same notation) for same ω_{de} and Ω_m^0 s.

Even though the value of D_{bp} at any epoch a is very close to that of D_g , its evolution behavior is quite different from that of D_g . We show this in Fig. 3. In the left panel of Fig. 3, the dashed and solid lines correspond to $|D_g - D_{\text{bp}}|/D_g \times 100$ % where D_{bp} with \mathcal{A} given in Eq. (3.8) when $\Omega_m^0 = 0.2$ and 0.3 for $\omega_{\text{de}} = -0.8$. Even though the error in D_{bp} at present is about 3 %, there is the discrepancy in cosmological evolution behaviors of D_g and D_{bp} . This discrepancy is clear when we compare the growth index f and f_{bp} as shown in the right panel of Fig. 3. Again the dashed and solid lines describe $|f - f_{\text{bp}}|/f \times 100$ % for the same values of Ω_m^0 s and ω_{de} as in the left panel of Fig. 3. The error in f_{bp} is more than 20 % at present.

As we show in Figs. 2 and 3, one might be able to obtain the value of the growth factor with small error from the approximate analytic solutions of the growth factor. However, one needs to pay attention when one considers the growth index. Especially, D_{bp} might not be used to compare with observations because of the incorrect behavior of f_{bp} obtained from the approximate analytic solution D_{bp} for some DE models.

We also compare the sub-horizon growth factor obtained from the Eq. (2.5) with the exact numerical one obtained from the numerical code, CMBFAST [58]. As we show in the Fig. 4, the relative errors of analytic sub-horizon growth factor is less than 1.5 % when we consider $a \geq 0.6$ in almost all interest cases. The square, circle, triangle, and diamond dots represent the relative error of analytic solution in Eq. (2.9) compared to the one obtained from CMBFAST when $\omega_{\text{de}} = -0.9, -1.0, -1.1,$ and -1.2 , respectively. We use the numerical solution at wavenumber $k = 0.09h\text{Mpc}^{-1}$. The result does not change for the other sub-horizon scale numerical solutions.

We obtain the analytic solutions for D_g and f that are exact for any DE model. And these solutions give the exact theoretical values of observable quantities. However, the exact solutions

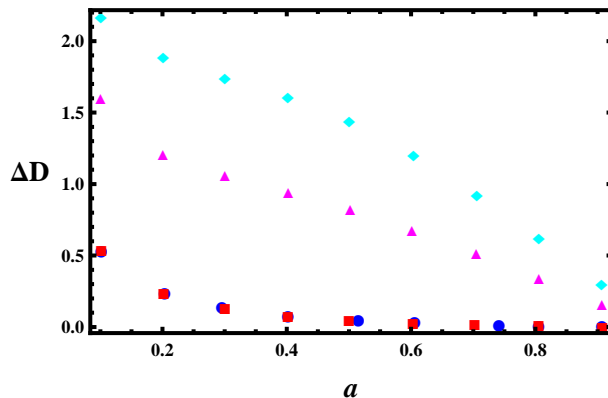


Figure 4: The relative errors of the analytic sub-horizon growth factor compared to the numerical one obtained from the CMBFAST. The square, circle, triangle, and diamond dots represent the relative errors when $\omega_{\text{de}} = -0.9, -1.0, -1.1,$ and $-1.2,$ respectively.

are limited to the constant values of ω_{de} . Thus, we need to investigate the generalization of the solutions to more general cases including time-varying ω_{de} . We will explain the possible extensions of them in the following section.

4 Applications for $D_g(a)$ and $f(a)$ to time-varying ω_{de}

It is well known that the time-dependence of ω_{de} is extremely difficult to discern because the dark energy is dynamically unimportant at the redshifts where ω_{de} departs from its low z value. In addition, for the substantial changes in ω_{de} at low redshift, there is always a constant ω_{de} that produces very similar evolution of all of the observables simultaneously [62, 63]. Also this analytic solution can provide useful templates to study the structure growth in dark energy models with time varying equation of state. The analytic solution is also very useful when one calculates the abundance of galaxy clusters as a function of redshift.

Even though the growth factor obtained in Eq. (2.9) is only true for the constant ω_{de} , we are able to apply this solution to the time-varying ω_{de} by interpolating between models with constant ω_{de} [17, 18, 19, 20]. For this purpose, we choose the sum of the step functions θ of $\omega_{\text{de}}(a)$ to probe the evolutions of $D_g(a)$ and $f(a)$,

$$\omega_{\text{de}}^{\text{step}}(a) = \sum_j \omega_{\text{de}}(j)\theta(a - a_j), \quad (4.1)$$

where $\omega_{\text{de}}(j)$ is the arbitrary value we need to fit from the background evolution observations. We use a specific model of this, $\omega_{\text{de}}^{\text{step}} = -0.8\theta(a) - 0.1\theta(a - 0.6) - 0.1\theta(a - 0.7)$, for the demonstration as shown in Fig. 5. The values of $\omega_{\text{de}}(j)$ and a_j are related to the values of the ω_{de} parameterization

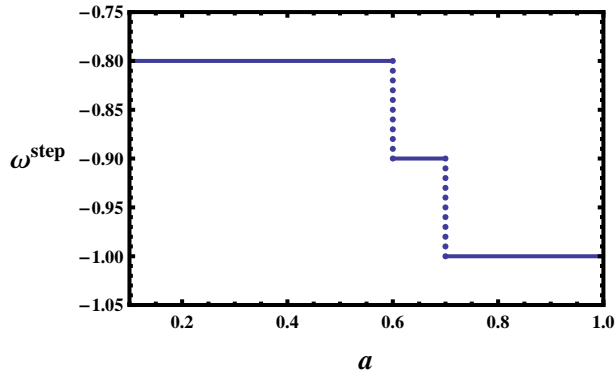


Figure 5: A specific model of Eq. (4.1).

$0.1 \leq a \leq 0.6$		$0.6 \leq a \leq 0.7$		$0.7 \leq a \leq 1.0$	
$D_g(0.1)$	$\frac{dD_g}{da} _{0.1}$	$D_g(0.6)$	$\frac{dD_g}{da} _{0.6}$	$D_g(0.7)$	$\frac{dD_g}{da} _{0.7}$
0.1	1	0.530531	0.661798	0.592623	0.579974
c_1	c_2	c_1	c_2	c_1	c_2
1.09339	-1.39169	1.04914	-1.07846	1.01286	-0.872337

Table 3: c_1 and c_2 are the values of the coefficients obtained from $D(a = a_j)$ and $\frac{dD(a)}{da}|_{a=a_j}$ at each interval.

which produce the proper background evolution like $H(a)$ [19]. Also, one is able to extend this parametrization to more general cases by putting more steps and/or different values of $\omega_{\text{de}}(j)$.

The advantages of this parametrization of ω_{de} are the followings. Even though the EOS is a discontinuous function of a (*i.e.* z), the physical quantities like $H(a)$, $D_g(a)$, and $f(a)$ obtained from this $\omega_{\text{de}}^{\text{step}}$ are smooth functions [17]. We are able to obtain the smooth functions $D_g(a)$ and $f(a)$ by solving for the proper values of c_1 and c_2 in Eq. (2.9) at each interval. This is shown in Tab. 3. Also the observations constrain the physical quantities in the specific interval of a . Thus, the parameterization of ω_{de} in Eq. (4.1) is a good one to probe the properties of ω_{de} when compared to the observations.

We show the cosmological evolutions of D_g and f in Fig. 6 for the different DE models. The evolutions of the growth factors D_g for $\omega_{\text{de}} = -1.0$, $\omega_{\text{de}}^{\text{step}}$, and -0.8 are described as dotted, solid, and dashed lines, respectively in the left panel of Fig. 6. The present values of D_g are (0.7797, 0.7328, 0.7327) for $\omega_{\text{de}} = -1.0$, $\omega_{\text{de}}^{\text{step}}$, and -0.8 , respectively. The evolutions of the D_g

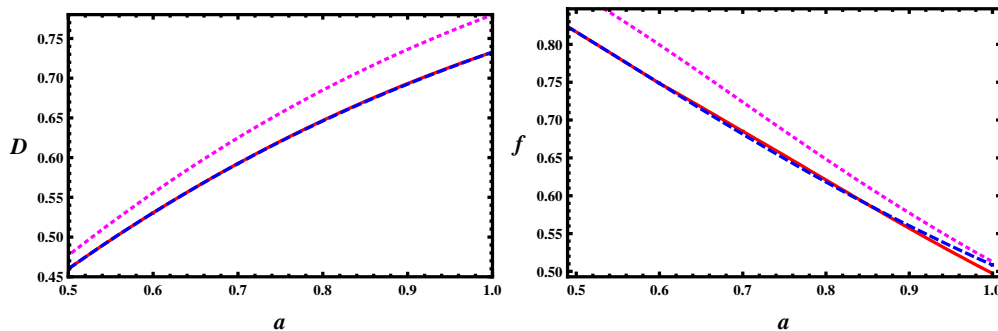


Figure 6: a) Cosmological evolutions of $D_g(a)$ for $\omega_{\text{de}} = -1.0$, $\omega_{\text{de}}^{\text{step}}$, and -0.8 (from top to bottom) when $\Omega_{\text{m}}^0 = 0.3$. b) Evolutions of $f(a)$ for $\omega_{\text{de}} = -1.0$, -0.8 , and $\omega_{\text{de}}^{\text{step}}$ (from top to bottom) for $\Omega_{\text{m}}^0 = 0.3$.

for $\omega_{\text{de}}^{\text{step}}$ and $\omega_{\text{de}} = -0.8$ are quite similar to each other because of the specific choices for values of $\omega_{\text{de}}^{\text{step}}$ in Eq. (4.1). If we have the shorter period of $a_{j=1}$ for $\omega_{\text{de}} = -0.8$ in $\omega_{\text{de}}^{\text{step}}$, then we may have the different evolution of D_g from the different choices of $\omega_{\text{de}}^{\text{step}}$. Also the cosmological evolutions of f are depicted as the dotted, solid, and dashed lines for $\omega_{\text{de}} = -1.0$, -0.8 , and $\omega_{\text{de}}^{\text{step}}$, respectively in the right panel of Fig. 6. We obtain the present values of f , (0.5128, 0.5084, 0.4974) when $\omega_{\text{de}} = -1.0$, -0.8 , and $\omega_{\text{de}}^{\text{step}}$, respectively. Thus, we obtain very interesting features of D_g and f from these DE models. Even though the present values of $\omega_{\text{de}} = -1.0$ and $\omega_{\text{de}}^{\text{step}}$ are equal, the evolution behaviors of D_g and f are quite different for these two models as shown in Fig. 6. $D(a=1)$ values are different by as large as 6 % and the difference in $f(a=1)$ is about 3 %. Thus, we may have a good chance to tell whether ω_{de} is a constant or not by investigating $D_g(a)$ and $f(a)$ at different a intervals.

5 Conclusion and discussion

We have analyzed the properties of the exact analytic solution of sub-horizon scale matter density perturbation (*i.e.* growth factor) for the general dark energy models with its equation of state ω_{de} being constant. From the comparison of this solution D_g with the well known approximate analytic solution D_g^{sw} , we have found that D_g^{sw} is a good approximate solution of D_g for the concordance model. D_g can be expressed with the slightly different functional forms for the specific values of ω_{de} . Especially, we have explicitly shown the alternative forms of D_g when $\omega_{\text{de}} = -1$ and $-\frac{1}{3}$. The two solutions in Refs. [54] and [56] are equivalent when $\omega_{\text{de}} = -1$ or $-\frac{1}{3}$ even though they look quite different.

We have scrutinized the several well known approximate analytic forms of the growth factor.

D_{cpt} is the one with the dark energy being the cosmological constant and D_{bp} is the extension of D_{cpt} for the general dark energy models with constant ω_{de} . f_{cpt} and f_{bp} are the growth indices obtained from D_{cpt} and D_{bp} , respectively. When the dark energy is the cosmological constant, D_{cpt} and f_{cpt} are very close to the correct D_g and f . However, D_{bp} and f_{bp} show the discrepancies with the correct D_g and f for some dark energy models. Especially, the error in f_{bp} for $\omega_{\text{de}} = -0.8$ and $\Omega_{\text{m}}^0 = 0.3$ is as large as 20% at present.

The approximate analytic solution D_{sw} , the approximate analytic forms D_{cpt} and D_{bp} are good approximate solutions of the exact D_g for the concordance model. However, all of them show some discrepancies with the correct D_g for some DE models and/or Ω_{m}^0 values. Thus, one needs to be very careful when one extends the approximate solutions to the general models and/or other cosmological parameters.

Even though we have obtained the exact analytic solution of D_g for the general DE models, this solution is limited to the constant ω_{de} models. Thus, the applications of this solution to the real observations are very limited. However, we can apply this solution to the more general cases like the time-varying ω_{de} by interpolating between models with constant ω_{de} . We have found that D_g and f obtained from the constant ω_{de} and the time-varying one are quite different even though we have the same values of ω_{de} s at present. If we are able to obtain a good constraint on ω_{de} from the cosmological background evolution observations, then we will be able to constrain D_g and f very accurately. Thus, the exact analytic solution of D_g can be used as the very useful tool for the interpretation of LSS survey data.

Acknowledgments

This work was supported in part by the National Science Council, Taiwan, ROC under the Grants NSC 95-2112-M-001-052-MY3 (KWN) and the National Center for Theoretical Sciences, Taiwan, ROC.

References

- [1] A. G. Riess *et al.*, *Astron. J.* **116**, 1009 (1998) [arXiv:astro-ph/9805201].
- [2] S. Perlmutter *et al.*, *Astrophys. J.* **517**, 565 (1999) [arXiv:astro-ph/9812133].
- [3] A. G. Riess *et al.*, *Astrophys. J.* **659**, 98 (2007) [arXiv:astro-ph/0611572].
- [4] E. V. Linder, *Am. J. Phys.* **76**, 197 (2008) [arXiv:0705.4102].
- [5] J. P. Ostriker and P. J. Steinhardt, [arXiv:astro-ph/9505066].
- [6] U. Seljak *et al.*, *Phys. Rev. D* **71**, 103515 (2005) [arXiv:astro-ph/0407372].

- [7] K. Yahata *et al.*, Publ. Astron. Soc. Jap. **57**, 529 (2005) [arXiv:astro-ph/0412631].
- [8] S. Cole *et al.*, Mon. Not. R. Astron. Soc. **362**, 505 (2005) [arXiv:astro-ph/0501174].
- [9] M. Tegmark *et al.*, Phys. Rev. D **74**, 123507 (2006) [arXiv:astro-ph/0608632].
- [10] E. Komatsu *et al.*, Astrophys. J. Suppl. **180**, 330 (2009) [arXiv:0803.0547].
- [11] V. B. Johri and P. K. Rath, Int. J. Mod. Phys. D **16**, 1581 (2007) [arXiv:astro-ph/0510017].
- [12] Y. Wang and M. Tegmark, Phys. Rev. Lett. **92**, 241302 (2004) [arXiv:astro-ph/0403292].
- [13] A. Upadhye, M. Ishak, and P. J. Steinhardt, Phys. Rev. D **72**, 063501 (2005) [arXiv:astro-ph/0411803].
- [14] P. J. E. Peebles and B. Ratra, Rev. Mod. Phys. **75**, 559 (2003) [arXiv:astro-ph/0207347].
- [15] L. Wang, R. R. Caldwell, J. P. Ostriker, and P. J. Steinhardt, Astrophys. J. **530**, 17 (2000) [arXiv:astro-ph/9901388].
- [16] R. Dave, R. R. Caldwell, and P. J. Steinhardt, Phys. Rev. D **66**, 023516 (2002) [arXiv:astro-ph/0206372].
- [17] W. Lee and K.-W. Ng, Phys. Rev. D **67**, 107302 (2003) [arXiv:astro-ph/0209093].
- [18] W. J. Percival, Astron. Astrophys. **443**, 819 (2005) [arXiv:astro-ph/0508156].
- [19] M. Barnard, A. Abrahamse, A. Albrecht, B. Bozek, and M. Yashar, Phys. Rev. D **78**, 043528 (2008) [arXiv:0804.0413].
- [20] J. Tang, F. B. Abdalla, and J. Weller, [arXiv:0807.3140].
- [21] J. Frieman, M. Turner, and D. Huterer, Ann. Rev. Astron. Astrophys. **46**, 385 (2008) [arXiv:0803.0982].
- [22] U. Alam, V. Sahni, T. D. Saini, and A. A. Starobinsky, Mon. Not. R. Astron. Soc. **344**, 1057 (2003) [arXiv:astro-ph/0303009].
- [23] E. V. Linder and A. Jenkins, Mon. Not. R. Astron. Soc. **346**, 573 (2003) [arXiv:astro-ph/0305286].
- [24] M. Kunz and D. Sapone, Phys. Rev. Lett. **98**, 121301 (2007) [arXiv:astro-ph/0612452].
- [25] M. Tegmark, Lect. Notes. Phys. **646**, 169 (2004) [arXiv:astro-ph/0207199].
- [26] L. Amendola, C. Quercellini, and E. Giallongo, Mon. Not. R. Astron. Soc. **357**, 429 (2005) [arXiv:astro-ph/0404599].

- [27] E. V. Linder, Phys. Rev. D **72**, 043529 (2005) [arXiv:astro-ph/0507263].
- [28] Y. Wang, JCAP **0805**, 021 (2008) [arXiv:0710.3885].
- [29] H. Zhan, L. Knox, and A. J. Tyson, Astrophys. J. **690**, 923 (2009) [arXiv:0806.0937].
- [30] R. R. Caldwell, R. Dave, and P. J. Steinhardt, Astrophys. Space. Sci. **261**, 303 (1998).
- [31] R. R. Caldwell, R. Dave, and P. J. Steinhardt, Phys. Rev. Lett. **80**, 1582 (1998) [arXiv:astro-ph/9708069].
- [32] C.-P. Ma, R. R. Caldwell, P. Bode, and L. Wang, Astrophys. J. **521**, L1 (1999) [arXiv:astro-ph/9906174].
- [33] M. Doran, C. M. Mueller, G. Schaefer, and C. Wetterich, Phys. Rev. D **68**, 063505 (2003) [arXiv:astro-ph/0304212].
- [34] J. K. Erickson, R. R. Caldwell, P. J. Steinhardt, C. Armendariz-Picon, and V. Mukhanov, Phys. Rev. Lett. **88**, 121301 (2002) [arXiv:astro-ph/0112438].
- [35] R. Bean and O. Doré, Phys. Rev. D **69**, 083503 (2004) [arXiv:astro-ph/0307100].
- [36] S. Hannestad, Phys. Rev. D **71**, 103519 (2005) [arXiv:astro-ph/0504017].
- [37] T. Koivisto and D. F. Mota, Phys. Rev. D **73**, 083502 (2006) [arXiv:astro-ph/0512135].
- [38] S. Lee, G.-C. Liu, and K.-W. Ng, Phys. Rev. D **73**, 083516 (2006) [arXiv:astro-ph/0601333].
- [39] M. Bartelmann, [arXiv:0906.5036].
- [40] P. J. E. Peebles, *Large-Scale Structure of the Universe* (Princeton University Press, 1980).
- [41] P. J. E. Peebles, Astrophys. J. **284**, 439 (1984).
- [42] O. Lahav, P. B. Lilje, J. R. Primack, and M. J. Rees, Mon. Not. R. Astron. Soc. **251**, 128 (1991).
- [43] D. J. Heath, Mon. Not. R. Astron. Soc. **179**, 351 (1977).
- [44] S. M. Carroll, W. H. Press, and E. L. Turner, ARA&A **30**, 499 (1992).
- [45] S. Basilakos, Astrophys. J. **590**, 636 (2003) [arXiv:astro-ph/0303112].
- [46] L. Wang and P. J. Steinhardt, Astrophys. J. **508**, 483 (1998) [astro-ph/9804015].
- [47] V. Silveira and I. Waga, Phys. Rev. D **50**, 4890 (1994).
- [48] L. Verde *et al.*, Mon. Not. R. Astron. Soc. **335**, 432 (2002) [arXiv:astro-ph/0112161].

- [49] E. Hawkins *et al.*, Mon. Not. R. Astron. Soc. **346**, 78 (2003) [arXiv:astro-ph/0212375].
- [50] P. McDonald *et al.*, Astrophys. J. **635**, 761 (2005) [arXiv:astro-ph/0407377].
- [51] N. P. Ross *et al.*, Mon. Not. R. Astron. Soc. **381**, 537 (2007) [arXiv:astro-ph/0612400].
- [52] J. da Angela *et al.*, [arXiv:astro-ph/0612401].
- [53] L. Guzzo *et al.*, Nature **451**, 541 (2008) [arXiv:0802.1944].
- [54] S. Lee and K.-W. Ng, [arXiv:0905.1522].
- [55] S. Lee, [arXiv:0905.4734].
- [56] S. Lee and K.-W. Ng, Phys. Lett. B **688**, 1 (2010) [arXiv:0906.1643].
- [57] S. Lee, [arXiv:0906.3066].
- [58] <http://www.cmbfast.org>.
- [59] W. B. Bonnor, Mon. Not. R. Astr. Soc. **117**, 104 (1957).
- [60] P. M. Morse and H. Feshbach, *Methods of Theoretical Physics, Part I* (McGraw-Hill Science, New York, 1953).
- [61] S. Dodelson, *Modern Cosmology* (Academic Press, San Diego, 2002) Erratum-ibid.
- [62] J. Kujat, A. M. Linn, R. J. Scherrer, and D. H. Weinberg, Astrophys. J. **572**, 1 (2002) [arXiv:astro-ph/0112221].
- [63] I. Maor, R. Brustein, J. McMahon, and P. J. Steinhardt, Phys. Rev. D **65**, 123003 (2002) [arXiv:astro-ph/0112526].